

Coarsening dynamics of three dimensional levitated foams: from wet to dry

N. Isert,¹ G. Maret,¹ and C.M. Aegerter²

¹*Fachbereich Physik, University of Konstanz, Universitätsstrasse 10, 78457 Konstanz, Germany*

²*Physik-Institut, University of Zürich, Winterthurerstrasse 190, 8057 Zürich, Switzerland*

(Dated: November 19, 2021)

We study diamagnetically levitated foams with widely different liquid fractions. Due to the levitation, drainage is effectively suppressed and the dynamics is driven by the coarsening of the foam bubbles. For dry foams, the bubble size increases as the square root of foam age, as expected from a generalized von Neumann law. At higher liquid content, the behavior changes to that of Ostwald ripening where the bubbles grow with the $1/3$ power of the age. Using Diffusing Wave Spectroscopy we study the local dynamics in the different regimes and find diffusive behavior for dry foams and kinetic behavior for wet foams.

PACS numbers: 83.80.Iz, 05.70.Ln, 83.85.Ei, 64.75.Cd

Foams are models of soft matter consisting of gas bubbles enclosed in a liquid, which have solid properties due to surface tension of the bubbles and their inside pressure [1]. Depending on the amount of liquid in the foam, bubbles can either be in contact or separated. In the former most common case of "dry" or "almost dry" foams, bubbles are substantially deformed and the thin flat liquid films in the contact area between them provide substantial mechanical stability to the foam [1]. "Wet" foams are less stable because the rather homogeneous mixture of separated bubbles is rapidly destroyed by flows due to buoyancy pushing bubbles upwards [1]. In "wet" and "almost dry" foams the dynamics is thus driven by the drainage of liquid between the bubbles due to gravity [2]. However, additional dynamics occurs even without drainage because of gas exchange between bubbles [3] due to the Laplace pressure $\Delta p = 2\sigma/r$ with r being the bubbles radius of curvature and σ the liquid-gas surface tension [4]. As a consequence, the average bubble size increases with time because of the lower gas pressure in the larger bubbles. This process, known as coarsening, has been described by von Neumann [5] and has been experimentally observed in two dimensional foams [3] as well as for very dry foams [6].

Here, we study three dimensional foams, which are levitated by a strong magnetic field gradient [7, 8]. Due to the diamagnetism of water, it is possible to effectively suppress the buoyancy of the gas bubbles and thus stabilize the foam against drainage even at high liquid content. With this simple trick it becomes possible to study the coarsening dynamics in 3D foams without chemical stabilizers for dry as well as wet foams over many hours in the laboratory. Without levitation such foams would decay within minutes on earth [9] which is why major efforts are under way to investigate them at conditions of steady microgravity at the ISS [10].

In dry foams the exchange of gas between bubbles takes place directly through the thin liquid films separating the bubbles. Because the rate of exchange is governed by the (Laplace-)pressure Δp , the growth rate of a bubble, i.e.

the current density of gas exchange, is proportional to the inverse of its radius, i.e. $j = \frac{dV}{A dt} \propto dr/dt \propto 1/r$. Here, A is the contact area of a bubble which is of order r^2 and V its volume. Given this dynamics, one obtains that the average size of bubbles will increase with time as $\langle r \rangle \propto t^{1/2}$. This can also be derived more strictly, as for instance done in [11]. When the bubbles are no longer in contact, it can be surmised that the mechanism of gas exchange between bubbles will have to change. In fact, the exchange of gas will now have to be achieved via diffusion in the liquid and the difference of the gas pressure in the bubbles to the saturation pressure in the liquid. Here, the diffusive current density $j \propto dr/dt$ will be determined by the gradient of the concentration, i.e. pressure difference. This means that we obtain $j \propto dr/dt \propto dp/dr$. Again using the fact that the pressure inside the bubbles is given by Laplace's law, we obtain $dr/dt \propto 1/r^2$ and hence a growth of the form $\langle r \rangle \propto t^{1/3}$. Again, this can be derived studying the detailed dynamics [12]. This qualitatively different type of coarsening is also known as Ostwald ripening and is for instance observed in the dynamics of the growth of inclusions in solids [13]. Since the nature of the dynamics changes when the bubbles are no longer in contact, the boundary between the two regimes is expected to be at a liquid fraction of $\sim 30\%$, which corresponds to the inverse density of closely packed spheres [14]. Since levitated foams can be created with a varying amount of liquid and relative stability to drainage, these predictions can thus be tested experimentally with our setup.

In order to assess the growth of the foam bubbles with age inside the three dimensional foam, we use multiply scattered light transmitted through the foam [15]. The transport mean free path of light in the turbid medium of the foam has been found to be proportional to the bubble size [16, 17]. This holds both for dry foams, where scattering mainly takes place at the thin liquid films between bubbles as well as for liquid foams, where the scattering centers are the bubbles themselves. In addition, the transmitted diffuse light can be used to obtain in-

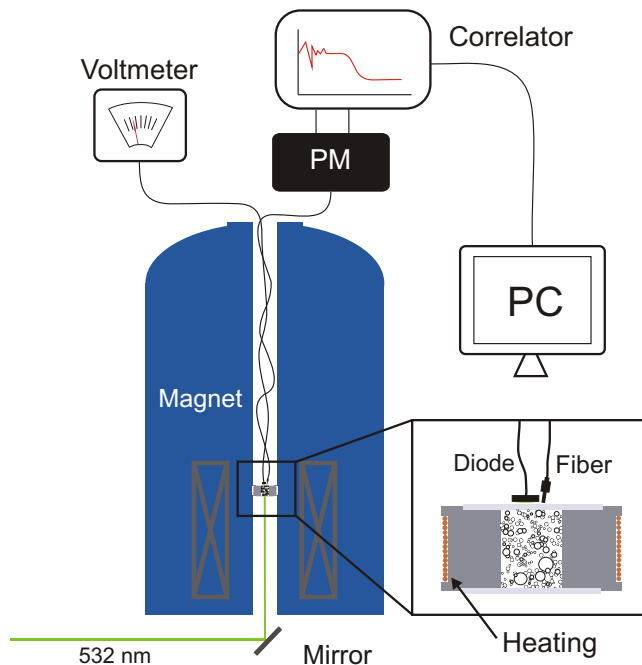


FIG. 1: Schematic illustration of the levitation setup. The foam sample cell, shown in detail in the inset, is placed inside the free bore of a 18 T cryomagnet, with optical access from above and below. From below, a CW laser is incident on the sample cell, whose transmission through the sample as a function of time is measured from above by a photodiode and an optical fibre connected to a photomultiplier and a correlator. For the determination of the integrated transmitted intensity, the photodiode is used, whereas the autocorrelation function from the correlator gives information about the dynamics discussed below. The inset shows details of the sample cell. Windows on top and bottom allow for optical access and a small coil in the side of the sample cell is used to heat the sample in the bore of the magnet, such that it is always kept at temperatures above 30°C .

formation on the averaged local dynamics of the foam via Diffusing Wave Spectroscopy (DWS) [18]. Here, the auto-correlation function of the multiply scattered light field directly provides the time dependence of the phase shift incurred by the dynamics of the scattering particles. Thus it is possible to determine whether the dynamics of the scatterers is diffusive or ballistic and from the respective time scales [19], the size of the dynamic particles can be obtained.

The foams used in the experiments consist of water, sodium dodecyl sulfate (SDS) as a surfactant and N_2 gas. The water-SDS mixture and the gas are put in two separate syringes, which are connected through a thin tube [20]. The water-SDS mixture is then transferred to the gas-filled syringe and the resulting mixture is transferred through the thin tube several times in order to achieve turbulent mixing. In this way an irregular foam with a

given mean pressure in the bubbles determined by the pressure on the syringes is obtained. The liquid content in the foam is determined by the volume-ratio of water-SDS mixture and gas in the initial state within the two syringes [20]. Due to the compression of the gas by the syringes, the effective liquid fraction of the foam will be somewhat higher than the initial composition given by the content in the two syringes. An initial liquid fraction of 25% corresponds roughly to an effective liquid fraction of 30%. The foam thus created is then transferred to a sample-cell of a diameter of 1.7 cm and a height of 1.2 cm, which is placed inside the room temperature bore of a superconducting magnet capable of applying a field of 18 T. Due to the insufficient thermal insulation of the bore and the high freezing point of a water-SDS mixture, a small heating coil is added around the sample cell in order to keep the foam at constant temperature all times (see Fig. 1). The magnet is a superconducting solenoid at the end of which the field shows a substantial gradient [21]. This means that there is a significant upward force on the diamagnetic water-SDS mixture, given by $f = \chi B \partial B / \partial z$, where f is the force density and χ is the diamagnetic susceptibility. At a specific point, when $B \partial B / \partial z = \rho g / \chi$, this force exactly compensates the gravitational force [7]. Due to the field distribution, this will lead to a stable levitation at this point [8], where the levitation will be homogeneous to one part in a thousand within a volume of 1 cm^3 , thus for almost the whole foam sample. Eliminating drainage this way opens up the possibility of observing the coarsening dynamics over extraordinary long times.

In order to study the dynamics, the foam is illuminated with a Coherent Verdi solid state CW laser at a wavelength of 532 nm and a power of 100 mW and the transmitted light is detected either with a photodiode or a glass fiber leading to a photomultiplier and a correlator card for DWS measurements [22]. The schematic setup is again shown in Fig. 1. Here, the auto-correlation function of fluctuating transmitted intensity is determined. These fluctuations are due to small movements of the scatterers (i.e. the foam bubbles), which lead to a change in the interference pattern of different multiple scattering paths through the sample [18]. This means that the correlation time gives a measure of the scatterer movement via the mean square fluctuations in the phase of the light induced by these movements.

In the multiple scattering regime, the transmitted intensity is given by Ohm's law, i.e. $T \propto l^* / L$ [15], where L is the thickness of the sample, l^* is the transport mean free path. Thus by determining the average transmitted intensity, we can directly obtain a measure of the change of the mean free path l^* with foam age, since both the sample thickness and the incident intensity are fixed. The mean free path of light in the sample has been shown before to give a determination of the bubble size with $l^* \propto r$ [23]. In figure 2, this dependence of l^* with

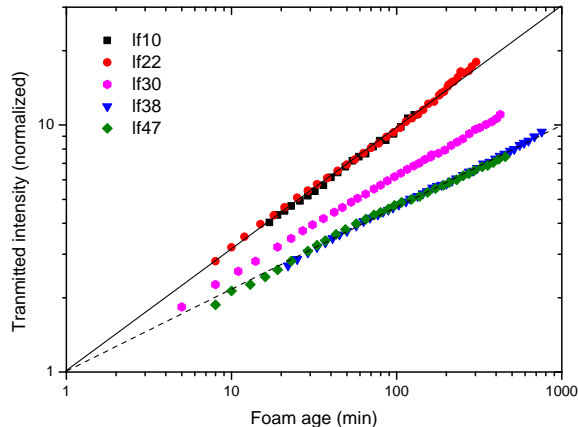


FIG. 2: The overall size evolution of the bubbles of a levitated foam are determined via the mean free path, l^* , as a function of foam age. In the limit of small absorption, the transmitted intensity, which is plotted here is directly proportional to l^* . Moreover, it has been shown that l^* in a foam is proportional to the bubble size [23], such that a temporal evolution of the transmitted intensity can be used to study the bulk coarsening dynamics directly. Here we show five examples of foams at different liquid fractions, showing different scaling behavior of l^* . As can be seen in foams with liquid content above 30% the bubbles increase in size more slowly, whereas at lower liquid fraction they increase faster. Above and below a narrow transition region, the behavior is however independent of liquid fraction. The slope in this double logarithmic plot directly gives the scaling exponent of the coarsening dynamics. Straight lines with a slope of $1/2$ (solid) and $1/3$ (dashed) are added for comparison.

foam age is shown for a set of foams with different liquid content. As can be seen in this double logarithmic plot, all foams show a scaling behavior with a power law increase of bubble size with age. For dry foams, this increase is faster with an exponent close to $1/2$, whereas for wet foams it is slower with an exponent close to $1/3$. These exponents are the asymptotic dynamics of the theoretical predictions for foam dynamics in the dry and wet case respectively [5, 12]. In the transition region, there is an intermediate behavior, where two distinct regimes can be seen corresponding to the two different dynamics.

These results are summarized in Fig. 3, where the exponents fitted for all experiments within a large range of liquid fractions is plotted. It can be clearly seen that below a liquid fraction of 25%, the exponents are all compatible with $1/2$, whereas above an initial liquid fraction of 30%, they are all compatible with $1/3$. Thus there is a clear transition in the coarsening behavior of the foams at a liquid fraction corresponding to the close packing of spheres. Both the transition as well as the values of the exponents are predicted by theory [5, 12].

Having observed this transition, it is interesting to

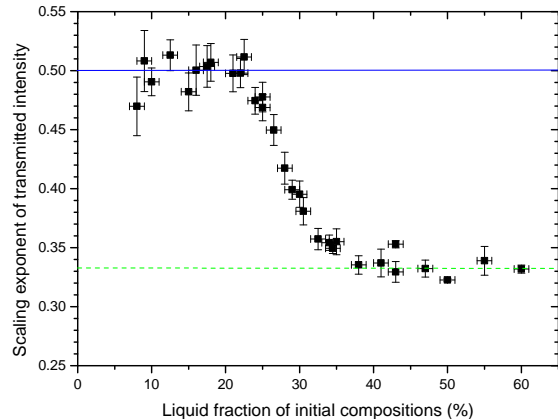


FIG. 3: Data similar to that shown in Fig. 2 but for a bigger variety of liquid fractions is summarized via the value of the scaling exponent as a function of the liquid fraction. At low liquid fractions, the exponent is in good accord with the von Neumann expectation of $1/2$, whereas for high liquid fractions it is consistent with the expectation of Ostwald ripening of $1/3$. The transition between these two regimes is rather narrow at liquid fractions between 25 and 30 %, as is expected for the point where separation of bubbles begins to occur.

investigate the difference in the local dynamics in the two different regimes more closely. For this purpose, we determine the mean square fluctuations of the scattering foam interfaces using DWS [19]. From the time auto-correlation function $g_2(t)$ of the transmitted intensity and the transport mean free path, we obtain $\log(g_2(t) - 1) \cdot T^2 \propto \langle \Delta r^2(t) \rangle$ on short time scales corresponding to the correlation time [19]. This is shown for foams of different wetness (i.e. initial liquid fraction) of 22%, 30% and 38%, in Fig. 4. The different $\langle \Delta r^2(t) \rangle$ shown for a single foam correspond to different ages of the foam, where each curve corresponds to a single data point in Fig.2. The evolution of aging time is indicated by the arrow and the ages for the different foams range from 8 to 303 min for 22% liquid fraction, 5 to 424 min for 30% liquid fraction and 9 to 755 min for 38% liquid fraction respectively. As can be seen, for dry foams, $\langle \Delta r^2(t) \rangle$ increases linearly with correlation time indicating a diffusive dynamics of the scatterers. The slope of the increase directly indicates the mobility of the scatterers, which can be seen to decrease with the age of the foam. This decrease corresponds to the increase in the average bubble size, in the same way as we have already seen from the mean free path above. For wet foams in contrast, the dynamics is rather independent of the age of the foam and the mean square fluctuations increase quadratically with time. This corresponds to a kinetic dynamics, where the scatterers travel ballistically during

the observed time. Moreover, the time scale of this kinetic dynamics is independent of the size of the bubbles, indicating that the bubbles move according to a convective flow.

In conclusion, using diamagnetically levitated foams not affected by drainage, we have shown the existence of a transition in the bulk coarsening dynamics of three dimensional foams at an effective liquid fraction of 30 %. At lower liquid fraction, the coarsening dynamics is governed by a von Neumann law [5, 11], which corresponds to a growth of the average bubble size with the square root of time. At higher liquid content, the bubbles grow via Ostwald ripening [12], i.e. the average bubble size grows with time to the power of 1/3. The difference in coarsening dynamics is driven by the fact that at low liquid content the bubbles are in close contact thus changing the nature of gas transport between bubbles.

In addition, we have shown that for wet foams, the local dynamics is kinetic, i.e. the bubbles essentially follow the convective flow of the interstitial liquid. The time scale of this dynamic correspondingly is independent of the age of the foam. Thus the DWS correlation time solely reflects the increase of the mean free path of light due to the increase in size.

For dry foams in contrast, where bubbles are closely packed, the dynamics of the bubbles is diffusive as would be expected in a dense system with many scattering centers. These movements are for instance induced by local events where bubbles move to relieve accumulated stresses. As the number of bubbles taking part in such rearrangements is constant [24], the size evolution of the bubbles can then also be obtained from the dynamics of these rearrangements. The time scale of these rearrangements also increases with the age of the foam as bigger bubbles move more slowly. In the future it will be interesting to characterize the dynamics of these rearrangements, which can give a complete picture of how local dynamics influences the global dynamics of the foam.

This work was funded by DFG in the context of the IRTG on Soft matter Physics as well as the Landestiftung Baden-Württemberg and the Swiss National Science Foundation.

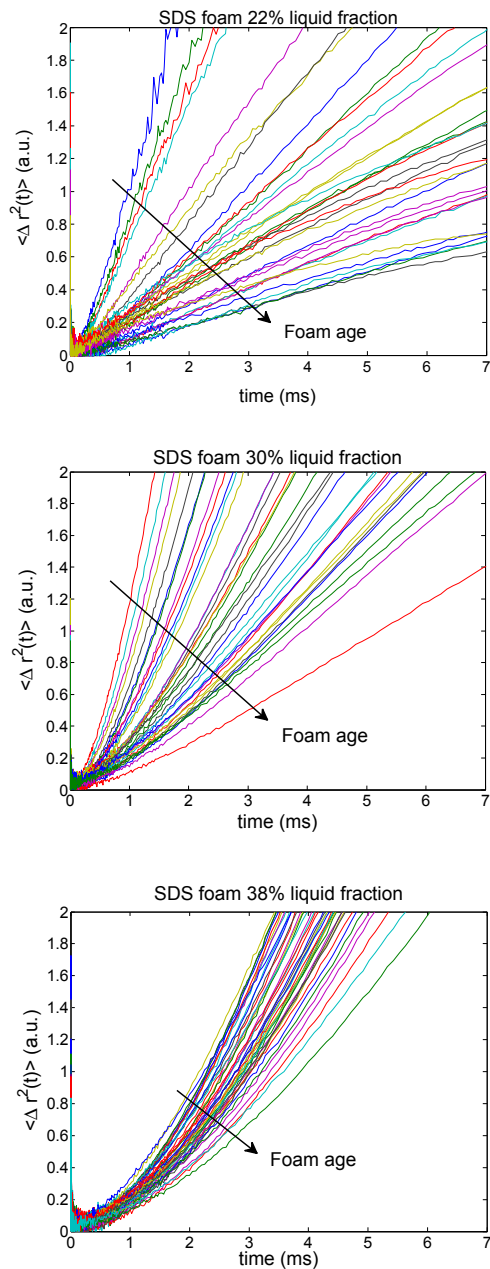


FIG. 4: The local dynamics of bubbles as studied by DWS for foams of different liquid fraction. a) shows a dry foam (22% lf), where the dynamics is diffusive as can be seen by the linear time evolution of the mean squared fluctuation of the scattering interfaces. The length scale corresponding to these fluctuations depends on the bubble size, thus the diffusivity of the scatterers decreases strongly with age of the foam. c) shows a wet foam above the transition (lf 38%). Here the increase is quadratic as corresponds to ballistic motion of the bubbles, presumably in convective flows induced by the heating. The dynamics of these flows does not depend much on the bubble size. b) Dynamics in the transition region (lf 30%). Here the dynamics of young foams is kinetic as the bubbles are separated at the beginning, however as the mean bubble size grows, their dynamics change to a more diffusive behavior, which also depends on the age of the foam.

-
- [1] D. Weaire and S. Hutzler, *The Physics of Foams*, Oxford Univ. Press (1999).
 - [2] S.A. Koehler *et al.*, Phys. Rev. E **58**, 2097 (1998).
 - [3] J.A. Glazier, S.P. Gross and J. Stavans, Phys. Rev. A **36**, 306 (1987).
 - [4] L.D. Landau and E.M. Lifshitz, *Course in theoretical Physics VI: Hydrodynamics*.
 - [5] J. von Neumann, in *Metal Interfaces* (C. Herring ed.), 108 (1952).
 - [6] C.P. Gonatas *et al.*, Phys. Rev. Lett. **75**, 573 (1995).
 - [7] W. Braunbeck, Z. Phys. **112**, 764 (1939).

- [8] M.V. Berry and A.K. Geim, *Europ. J. Phys.* **18**, 307 (1997).
- [9] R. Straub, Diploma thesis, Univ. Konstanz (2008).
- [10] A. Saint-Jalmes, S. Marze, M. Safouane and D. Langevin, *Microgravity sci. technol.* **XVIII**, 5 (2006).
- [11] R.D. MacPhearson and D.J. Srolovitz, *Nature (London)* **446**, 1053 (2007).
- [12] W. Ostwald, *Z. Phys. Chem.* **37**, 385 (1901); I.M. Lifshitz and V.V. Slyozov, *J. Phys. Chem. Solids* **19**, 35 (1961); C. Wagner, *Z. Elektr. Inf.-Energietechn.* **65**, 581 (1961).
- [13] A. Knaebel *et al.*, *Europhys. Lett.* **52**, 73 (2000).
- [14] N.J.A. Sloane, *Sci. Am.* **250**, 116 (1984).
- [15] P. Sheng, *Introduction to Wave Scattering, Localization and Mesoscopic Phenomena*, Academic Press (1995).
- [16] D.J. Durian, D.A. Weitz and D.J. Pine, *Phys. Rev. A* **44**, R7902 (1991).
- [17] S. Cohen-Addad and R. Höhler, *Phys. Rev. Lett.* **86**, 4700 (2001).
- [18] G. Maret and P.E. Wolf, *Z. Phys. B* **65**, 409 (1987).
- [19] D.J. Pine, D.A. Weitz, J.X. Zhu and E. Herbolzheimer, *J. Phys.* **51**, 2101 (1990).
- [20] A. Saint-Jalmes, M.U. Vera and D.J. Durian, *Europ. Phys. J. B* **12**, 67 (1999).
- [21] C.C. Maas, N. Isert, G. Maret and C.M. Aegerter, *Phys. Rev. Lett.* **100**, 248001 (2008).
- [22] G. Maret, *Curr. Op. Colloid Int. Sci.* **2**, 251 (1997).
- [23] A.S. Gittings, R. Bandyopadhyay and D.J. Durian, *Europhys. Lett.* **65**, 414 (2004).
- [24] A.S. Gittings and D.J. Durian, *Phys. Rev. E* **78**, 066313 (2008).